ANALYTICAL SOLUTION OF DAM BREAK WAVE WITH FLOW RESISTANCE. APPLICATION TO TSUNAMI SURGES

HUBERT CHANSON

Dept of Civil Engineering, The University of Queensland, Brisbane QLD 4072, Australia
(e-mail: h.chanson@uq.edu.au)

Abstract

Surge waves resulting from dam breaks have been responsible for numerous losses of life. Related situations include flash floods, debris flow surges, surging waves in the swash zone, and tsunami surges on dry coastal plains. Herein the dam break wave flow is analysed as a wave tip region where flow resistance is dominant, followed by an ideal-fluid flow region where inertial effects and gravity effects are dominant. The analytical development yields an explicit expression of the instantaneous free-surface profile and flow properties that compare well with well-known experimental data. Results are then applied to tsunami surges on dry coastal plains, and compared with some data set. The present development offers simple analytical expressions that compare well with both experimental data and more advanced theoretical solutions, and that are further well-suited for pedagogical purposes as well as computational model validation.

Keywords: Dam break wave; Analytical solution; Bed friction; Tsunami surge

1. INTRODUCTION

Surge waves resulting from dam breaks have been responsible for numerous losses of life. Related situations include flash floods, flood runoff in ephemeral streams, debris flow surges, surging waves in the swash zone, rising tides in dry estuaries and tsunami surges on dry coastal plains. In all cases, the surge front is a shock characterised by a sudden discontinuity and extremely rapid variations of flow depth and velocity. Albeit major "concerted" actions, there has been a lack of basic theoretical and physical studies for the past 40 years. For example, current knowledge of dam break wave surging down rough surfaces remains rudimentary and there are still some arguments of the unsteady turbulent flow fundamentals. Modern predictions of dam break wave rely too often on numerical predictions, validated with limited data sets.

A new theoretical analysis is developed herein and it yields new simple analytical solutions of the dam break wave on dry horizontal channel. The results are compared with both ideal-fluid solution and physical data obtained in large-size facilities. The solutions are then applied to tsunami surges and compared with preliminary data from the 26 December 2004 disaster.

2. BASIC EQUATIONS

A dam break wave results from a sudden release of a mass of fluid in a channel (Fig. 1). For one-dimensional applications and within some basic assumptions, the unsteady flow can be characterised at any point and time by two variables: e.g., V and d where V is the flow velocity and d is the water depth. The unsteady flow properties are described by a system of two partial differential equations:

$$\frac{\partial d}{\partial t} + \frac{A}{B} * \frac{\partial V}{\partial x} + V * \frac{\partial d}{\partial x} + \frac{V}{B} * \left(\frac{\partial A}{\partial x}\right)_{d=constant} = 0 \quad \text{Continuity equation} \qquad (1)$$

$$\frac{\partial V}{\partial t} + V * \frac{\partial V}{\partial x} + g * \frac{\partial d}{\partial x} + g * (S_f - S_o) = 0 \quad \text{Dynamic wave equation} \qquad (2)$$

where t is the tine, x is the streamwise co-ordinate, A is the cross-section area, B is the free-surface width, S_o is the bed slope ($S_o = \sin$), is the angle between the bed and the horizontal with > 0 for a downward slope, and S_f is the friction slope (e.g. Liggett 1994, Montes 1998, Chanson 2004). The friction slope is defined as : $S_f = f/2*V^2/(g*D_H)$ where D_H is the hydraulic diameter and the Darcy friction factor f is a non-linear function of both relative roughness and flow Reynolds number. The differential form of the Saint-Venant equations (i.e. Eq. (1) and (2)) cannot be solved directly usually because of non-linear terms and complicated functions. A mathematical technique to solve the system of partial differential equations is the method of characteristics. It yields a characteristic system of equations :

$$\frac{D}{Dt}(V + 2 * C) = - g * (S_f - S_o) \quad \text{forward characteristic} \qquad (3a)$$

$$\frac{D}{Dt}(V - 2 * C) = - g * (S_f - S_o) \quad \text{backward characteristic} \qquad (3b)$$

along:

$$\frac{d x}{dt} = V + C \quad \text{forward characteristic C1} \qquad (4a)$$

$$\frac{d x}{dt} = V - C \quad \text{backward characteristic C2} \qquad (4b)$$

where C is celerity of a small disturbance for an observer travelling with the flow: $C = \sqrt{g*d}$ for a rectangular channel.

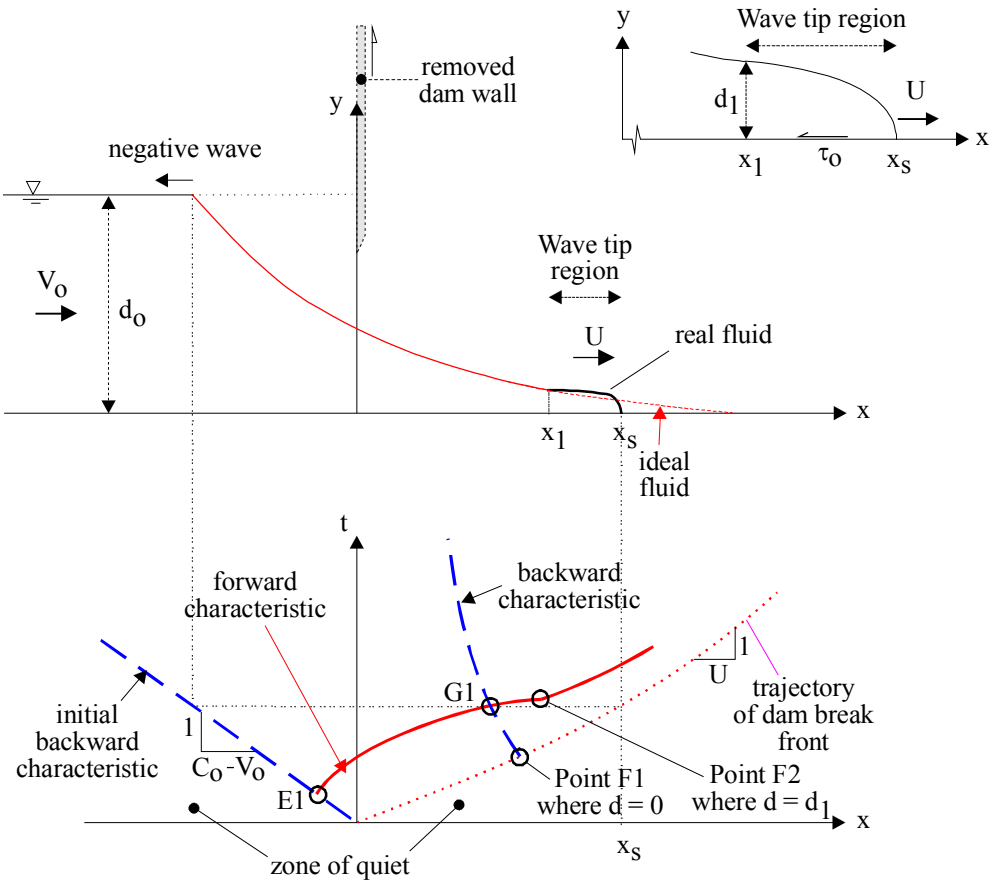

Fig. 1 Dam break wave in horizontal channel: definition sketch

2.1 IDEAL FLUID FLOW SOLUTION

Considering an ideal dam break surging over a dry, horizontal bed, the method of characteristics may be applied to solve completely the wave profile for a wide rectangular channel (Ritter 1892). Equations (3) and (4) may be simplified ($S_o = S_f = 0$) yielding the celerity of the wave front:

$$U = 2 * \sqrt{g * d_o} \tag{5}$$

where d_o is the initial reservoir height (Fig. 1). The instantaneous dam break creates a negative wave propagating upstream into a fluid at rest with a celerity $C_o = \sqrt{g*d_o}$ for a rectangular channel. At a given time t from the instantaneous dam removal, the free-surface profile between the leading edge of the negative wave and the wave front is a parabola:

$$\frac{x}{t * \sqrt{g * d_o}} = 2 - 3 * \sqrt{\frac{d}{d_o}} \quad \text{for} \quad -1 \leq \frac{x}{t * \sqrt{g * d_o}} \leq +2 \tag{6}$$

Equation (6) was first proposed by Barré de Saint-Venant (1871) for a frictionless surge in a horizontal channel. Although he assumed an initial downstream water depth, his reasoning is also valid for an initially-dry channel.

3. DAM BREAK IN A DRY HORIZONTAL CHANNEL WITH BED FRICTION

3.1 PRESENTATION OF THE DIFFUSIVE WAVE MODEL

For a dam break wave in dry horizontal channel with semi-infinite reservoir, initially at rest ($V_o = 0$), experiments showed that Ritter's theory is not valid to predict the flow properties at the leading tip of the wave front. Experimental measurements demonstrated that the wave front has a rounded shape and its celerity U is less than $2*C_o$ (e.g. Schoklitsch 1917, Dressler 1954, Cavaille 1965, Estrade 1967). These observations demonstrated further that the flow properties were well approximated by Ritter's theory between the most upstream extent of the initial backward characteristic and a flow region immediately behind the dam break wave-leading tip. Herein the dam break flow is analysed as an ideal-fluid flow region behind a flow resistance-dominated tip zone. The transition between ideal dam break wave profile and wave tip region is denoted F2 as shown in Figure 1. Point F2 is located at $x = x_1$ where the flow depth is d_1 and the velocity is V_1.

In the wave tip region ($x_1 \leq x \leq x_S$), flow resistance is dominant, and the acceleration and inertial terms are small. The flow velocity does not vary rapidly in the forward tip zone and experimental data showed that it is about the wave front celerity U (Dressler 1952,1954, Estrade 1967, Lauber 1997). The dynamic wave equation may be reduced into a diffusive wave equation:

$$\frac{\partial d}{\partial x} + \frac{f}{8} * \frac{U^2}{g*d} = 0 \quad \text{Wave tip region} \tag{7}$$

Next to the leading edge of the wave (i.e. $x \leq x_S$), the slope of the free-surface becomes important to counterbalance the flow resistance. The integration of the diffusive wave equation (Eq. (7)) yields the shape of the wave front:

$$\frac{d}{d_o} = \sqrt{\frac{f}{4} * \frac{U^2}{g * d_o} * \frac{x_S - x}{d_o}} \quad \text{Wave front profile} \tag{8}$$

assuming a constant Darcy friction factor f in the wave tip region (Chanson 2005a). Although the shape of the wave front is independent of time, both the wave front celerity U and location x_S are functions of t.

3.2 COMPLETE SOLUTION ($V_o = 0$)

The instantaneous dam break creates a negative wave propagating upstream into a still fluid with known water depth d_o. In the (x, t) plane, the initial negative wave characteristic has a slope $dt/dx = -1/C_o$ where $C_o = \sqrt{g*d_o}$. Note that the initial backward characteristic is a straight line, but the other backward characteristics are not. Forward characteristics can be drawn issuing from the initial backward characteristic for $t > 0$ (Fig. 1). Between the points E1 and F2, the flow properties satisfy the ideal dam break wave properties:

$$\sqrt{\frac{d}{d_o}} = \frac{1}{3} * \left(2 - \frac{x}{t * \sqrt{g * d_o}}\right) \quad -1 \leq \frac{x}{t * \sqrt{g * d_o}} \leq \frac{x_1}{t * \sqrt{g * d_o}} \tag{9a}$$

$$\frac{V}{\sqrt{g * d_o}} = \frac{2}{3} * \left(1 + \frac{x}{t * \sqrt{g * d_o}}\right) - 1 \leq \frac{x}{t * \sqrt{g * d_o}} \leq \frac{x_1}{t * \sqrt{g * d_o}} \quad (9b)$$

where d and V are the flow depth and velocity respectively at a distance x from the dam, and t is the time from the instantaneous dam removal.

In the wave tip region ($x_1 \leq x \leq x_S$), the flow depth in the wave tip region may be estimated using the solution of the diffusive wave equation taking into account flow resistance (i.e. Equation (8)). The free-surface and velocity must be continue at the point F2, and this yields a series of 4 equations in terms of its flow properties (x_1, V_1, d_1) and wave front location x_S. The conservation of mass must be further satisfied. The mass of fluid in the wave tip region (i.e. $x_1 \leq x \leq x_S$) must equal the mass of fluid in the ideal fluid flow profile for $x_1 \leq x \leq 2*\sqrt{g*d_o}*t$:

$$\int_{x_1}^{x_S} \sqrt{\frac{f}{4 * g} * U^2 * (x_S - x)} * dx = \int_{x_1}^{2*\sqrt{g*d_o}*t} \frac{1}{9 * g} * \left(2 * \sqrt{g * d_o} - \frac{x}{t}\right)^2 * dx \quad (10)$$

The exact solution in terms of the wave front celerity is:

$$\frac{8}{3} * \frac{1}{f} * \frac{\left(1 - \frac{1}{2} * \frac{U}{\sqrt{g * d_o}}\right)^3}{\frac{U^2}{g*d_o}} = \sqrt{\frac{g}{d_o}} * t \quad (11)$$

while the wave front location equals:

$$\frac{x_S}{d_o} = \left(\frac{3}{2} * \frac{U}{\sqrt{g * d_o}} - 1\right) * \sqrt{\frac{g}{d_o}} * t + \frac{4}{f * \frac{U^2}{g*d_o}} * \left(1 - \frac{1}{2} * \frac{U}{\sqrt{g*d_o}}\right)^4 \quad (12)$$

and the free-surface profile satisfies:

$$\frac{d}{d_o} = \frac{1}{9} * \left(2 - \frac{x}{t * \sqrt{g * d_o}}\right)^2 - \sqrt{\frac{g}{d_o}} * t \leq \frac{x}{d_o} \leq \left(\frac{3}{2} * \frac{U}{\sqrt{g * d_o}} - 1\right) * \sqrt{\frac{g}{d_o}} * t \quad (13a)$$

$$\frac{d}{d_o} = \sqrt{\frac{f}{4} * \frac{U^2}{g * d_o} * \frac{x_S - x}{d_o}} \left(\frac{3}{2} * \frac{U}{\sqrt{g * d_o}} - 1\right) * \sqrt{\frac{g}{d_o}} * t \leq \frac{x}{d_o} \leq \frac{x_S}{d_o} \quad (13b)$$

The location of point F2 is given by:

$$\frac{x_1}{\sqrt{g * d_o} * t} = \left(\frac{3}{2} * \frac{U}{\sqrt{g * d_o}} - 1\right) \quad (14)$$

The present development was successfully compared with experimental data in turbulent flows by Schoklitsch (1917), Dressler (1954), Faure and Nahas (1961), Cavaille (1965), Estrade (1967) and Lauber (1997). Some examples are presented in Figure 2 in terms of instantaneous free-surface profiles for different dimensionless times. In Figure 2A, the ideal fluid flow solution (Eq. (6)) is shown for comparison. The diffusive wave model was successfully compared with the theoretical developments of Dressler (1952) and Whitham

(1955). An extension of the model to laminar dam break wave was also compared qualitatively with the viscous flow data of Debiane (2000) (Chanson 2005a), and a complete solution for fully-rough turbulent motion is presented by Chanson (2005a).

3.3 DISCUSSIONS

Great care must be taken in the selection of the flow resistance coefficient. Since the water depth along the dam break wave ranges from zero at the wave front to the reservoir depth at the upstream end, friction factor estimates must be calibrated and validated with experimental data. For the comparative analyses conducted herein, the friction factor was found to be almost independent of time and experimental flow conditions for a given type of roughness. The results were further consistent between independent data sets (Chanson 2005a). This analysis showed that accurate calibrations of the flow resistance must be performed using instantaneous free-surface profiles. Alternate techniques based upon wave front location and celerity, or fixed-point measurements, might provide some order of magnitude only.

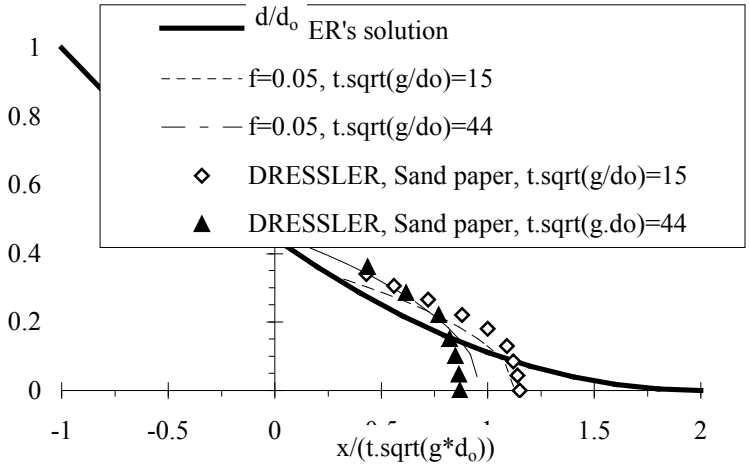

(A) Comparison with Dressler's (1954) data (L = 65 m, W = 0.225 m, sand paper invert)

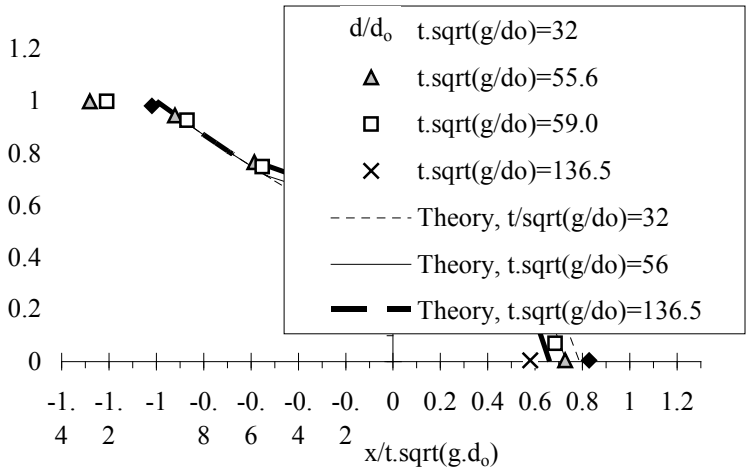

(B) Comparison with Cavaille's (1965) data (L = 40 m, W = 0.25 m, rough invert)

Fig. 2 Dimensionless free-surface profile solutions - Comparison with experimental data

The present method yields an explicit expression of the wave front celerity, wave front location and wave tip region characteristics. Equation (11) provides a direct relationship between the dimensionless wave front celerity $U/\sqrt{g*d_o}$ and dimensionless time $t*\sqrt{g/d_o}$. Equation (12) yields the dimensionless wave front location x_S/d_o as a function of the dimensionless wave front celerity. Equations (13) and (14) give the entire dimensionless free-surface profile d/d_o as a function of the dimensionless time. This simple system of linear equations provides a means to assess simply the effect of the flow resistance on the dam break wave propagation of real fluids.

The comparison between analytical results and theory shows that the diffusive wave approximation is reasonable for relatively small times after dam break. It might become less valuable when the wave tip region becomes large. It is also limited to a semi-infinite reservoir, and it assumes a constant Darcy-Weisbach friction factor in the wave tip region. A further limitation is the use of the Saint-Venant equations and their underlying assumptions (e.g. Chanson 2004). For example, the Saint-Venant equations are not valid during the initial instants following dam break.

3.4 DAM BREAK WITH NON-ZERO INITIAL VELOCITY (DIFFUSIVE WAVE MODEL)

The problem may be extended if the flow velocity behind the dam is V_o everywhere for $t < 0$ (Fig. 1). It is assumed that the translation of both dam and reservoir at the speed V_o is frictionless prior to dam removal, and that the translation of the undisturbed reservoir remains frictionless for $t \geq 0$. Dam removal takes place instantaneously at $t = 0$ when the dam is at $x = 0$. A development similar to the above yields an exact solution in terms of the wave front celerity:

$$\frac{8}{3} * \frac{1}{f} * \frac{\left(1 + \frac{1}{2} * \frac{V_o}{\sqrt{g * d_o}} - \frac{1}{2} * \frac{U}{\sqrt{g * d_o}}\right)^3}{\frac{U^2}{g*d_o}} = \sqrt{\frac{g}{d_o}} * t \tag{15}$$

while the wave front location equals:

$$\frac{x_S}{d_o} = \left(\frac{3}{2} * \frac{U}{\sqrt{g * d_o}} - \frac{1}{2} * \frac{V_o}{\sqrt{g * d_o}} - 1\right) * \sqrt{\frac{g}{d_o}} * t + \frac{4}{f * \frac{U^2}{g*d_o}} * \left(1 + \frac{1}{2} * \frac{V_o}{\sqrt{g*d_o}} - \frac{1}{2} * \frac{U}{\sqrt{g*d_o}}\right)^4 \tag{16}$$

and the free-surface profile satisfies:

$$\frac{d}{d_o} = 1 \text{ for } \frac{x}{d_o} \leq \frac{V_o - \sqrt{g*d_o}}{d_o} * t \tag{17a}$$

$$\frac{d}{d_o} = \frac{1}{9} * \left(2 + \frac{V_o}{\sqrt{g*d_o}} - \frac{x}{t * \sqrt{g * d_o}}\right)^2$$

$$\text{for } \frac{V_o - \sqrt{g*d_o}}{d_o} * t \le \frac{x}{d_o} \le \left(\frac{3}{2} * \frac{U}{\sqrt{g * d_o}} - \frac{1}{2} * \frac{V_o}{\sqrt{g * d_o}} - 1 \right) * \sqrt{\frac{g}{d_o}} * t \quad (17b)$$

$$\frac{d}{d_o} = \sqrt{\frac{f}{4} * \frac{U^2}{g * d_o} * \frac{x_S - x}{d_o}}$$

$$\text{for } \left(\frac{3}{2} * \frac{U}{\sqrt{g * d_o}} - \frac{1}{2} * \frac{V_o}{\sqrt{g * d_o}} - 1 \right) * \sqrt{\frac{g}{d_o}} * t \le \frac{x}{d_o} \le \frac{x_S}{d_o} \quad (17c)$$

$$\frac{d}{d_o} = 0 \text{ for } \frac{x_S}{d_o} \le \frac{x}{d_o} \quad (17d)$$

and the wave tip region length is:

$$\frac{x_S - x_1}{d_o} = \frac{4}{f} * \frac{g * d_o}{U^2} * \left(1 + \frac{1}{2} * \frac{V_o}{\sqrt{g * d_o}} - \frac{1}{2} * \frac{U}{\sqrt{g*d_o}} \right)^4 \quad (18)$$

Note that the results yield the results previously obtained for $V_o = 0$.

Fig. 3 Advancing mud and debris surge in Banda Aceh (26 December 2004 tsunami) - Looking upstream for four different times: (A) t = 8.48 s (B) t = 13.12 s (C) t = 16.0 s (D) t = 39.0 s

4. APPLICATION TO TSUNAMI SURGES

Simple applications of the above developments are presented in Chanson (2005a). One example is the tsunami surge runup on a flat coastline. A tsunami wave is a long-period wave generated by ocean bottom motion during an earthquake typically. Although the wave amplitude is moderate in the middle of the ocean (i.e. 0.5 to 1 m), the tsunami wave speed decreases near the shoreline with decreasing water depths. For a constant energy flux, the wave height increases accordingly until wave breaking occurs. Thereafter, the tsunami waters surge on dry or inundated coastal plains, in a manner somewhow similar to a dam break wave. Such tsunami surges were witnessed in Indonesia (Western Aceh, Band Aceh) and Thailand (Khao Lak, Patong) on 26 Dec. 2004 (Fig. 3). Fig. 3 shows an advancing surge front in a street of Banda Aceh. While the exact location is unknown, it is believed to be about 1.5 to 3 km inland. For a 100 m long stretch, the surge advanced with an average celerity U of about 1.5 to 1.6 m/s. However the advance was neither two-dimensional nor smooth. The surge appeared to progress section by section, in a somewhat disorganised manner. Although this behaviour might be induced by flow turbulence, it might also be related to the fluid rheology. The time variations of water depth were estimated at three different locations of the street, and the data are shown in Fig. 4, with the (bottom) horizontal axis being a time being measured from when the surge front reached the location and the (left) vertical axis is the flow depth in metres.

Table 1 - Tsunami surge application: analytical results at x = 2000 m for d_o =10.5 m (V_o = 0 & 12 m/s) - Comparison between ideal- and real-fluid flow calculations

Flow property at x = 2000 m	Case 1 Ideal fluid $V_o = 0$	Case 2 Ideal fluid V_o = 12 m/s	Case 3 Real fluid $V_o = 0$	Case 4 Real fluid V_o = 12 m/s
(1)	(2)	(3)	(4)	(5)
Surge arrival time since breaking (s) =	99	62	340	200
U (m/s) =	20.3	32.3	1.2	2.9

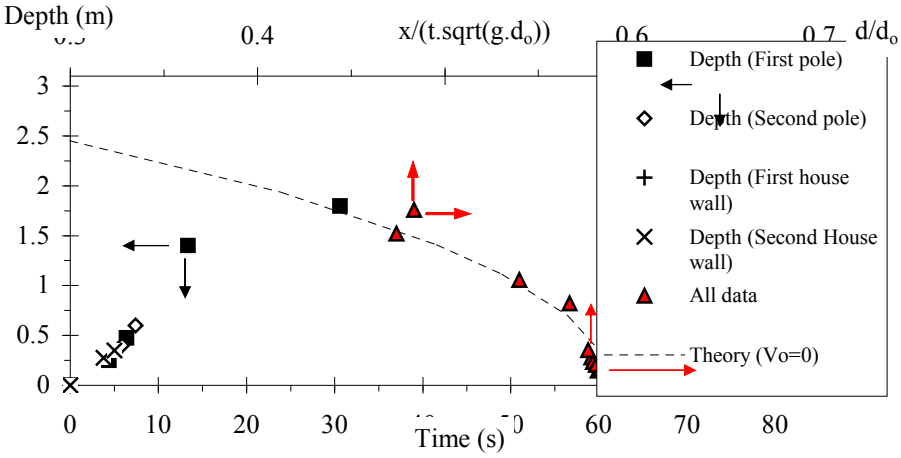

Fig. 4 Time-variations of the water depth for the surge shown in Figure 3 (Bottom and left axes) and dimensionless comparison with Equation (13) (Right and top axes)

The data were compared with the above theoretical development. Assuming a 1 m high tsunami wave generated in deep water (1,000 m), solitary wave calculations predict wave breaking near the shore with a maximum wave height of 10.5 m and a wave celerity at breaking of V_o = 12 m/s (Synolakis 1997, Chanson et al. 2000, Chanson 2005a). For similar conditions, dam break wave calculations were conducted for d_o = 10.5 m, V_o = 0 and 12 m/s, x = 2 km, and the flow resistance was assumed f = 0.5. Four cases were considered: ideal- and real-flows, with and without initial motion. Note that, for a reservoir height d_o = 10. 5 m, corresponding to the maximum wave height, the calculations yield a water depth at the end of the process of $4/9*d_o$ = 4.7 m that is close to maximum flooding heights in Banda Aceh (Tsuji 2005; Borrero 2005, *Person. Comm.*, Chanson 2005b). The predictive results are summarised in Table 1. Real fluid flow calculations highlighted the strong effect of bed resistance on wave propagation. The quantitative results in terms of surge front celerity were comparable with observations for the surge shown in Figure 3 and 4. Field observations were further compared with Equations (11) to (14) for the above conditions (d_o = 10.5 m, x = 2000 m). Results are presented in Figure 4 for the case V_o = 0. Both calculations (dotted line) and observed data (red triangles) are presented in dimensionless terms (top horizontal & right vertical axes). Fig. 4 shows a good agreement between data and theory in terms of the wave front shape.

5. REMARKS

A better agreement was obtained assuming no initial flow motion, while a relatively large flow resistance had to be considered. Further the calculations were dependent upon the initial flow conditions.

Although the above approach is very simplistic and relies upon basic assumptions, it is derived from basic principles and physically-based equations that were successfully validated with a wide range of physical data in large size facilities. The resulting set of equations provides a simple tool to predict tsunami surge and dam break wave propagation. Such calculations can be performed in real-time and provides very rapid information that may be vital in emergency situations.

6. DISCUSSIONS AND CONCLUDING REMARKS

The present work is focused on a simple solution of the dam break wave problem using the Saint-Venant equations and the method of characteristics. Analytical solutions are developed for an instantaneous dam break with a semi-infinite reservoir in a wide rectangular channel. The dam break wave flow is analysed as a wave tip region where flow resistance is dominant, followed by an ideal-fluid flow region where inertial effects and gravity effects are dominant. The analytical results were validated by successful comparisons between several experimental data sets obtained in large-size facilities and theoretical results in terms of instantaneous free-surface profiles, wave front location and wave front celerity. The former comparison with instantaneous free-surface data is considered to be the most accurate for the estimation of the flow resistance and the best validation technique. In the second part of the

paper, the analytical developments are applied to tsunami surges. The calculations are compared with observed surge data during the 26 December 2004 tsunami catastrophe. A reasonable agreement was observed in terms of surge front celerity and free-surface profile (Fig. 4). Such an approach may provide emergency services with accurate real-time predictions of tsunami flooding that may be vital in catastrophic situations.

The present development offers several advantages over existing methods. First the theoretical results for real-fluid flows yield simple explicit analytical expressions that compare well with experimental data and more advanced theoretical solutions. Second the proposed development is a simple pedagogical application of the Saint-Venant equations and method of characteristics, linking together the simple wave equations yielding Ritter's solution, with a diffusive wave equation for the wave tip region. Both the simple wave and diffusive wave equations constitute relatively simple lecture materials that may be introduced in advanced undergraduate subjects (e.g. Henderson 1966, Chanson 2004). Third, these explicit analytical solutions may be used to validate numerical solutions of the method of characteristics applied to the dam break wave problem. This is important in dam break wave calculations where the wave tip is a flow singularity with zero water depth. Further most numerical models must be calibrated in terms of flow resistance. Some comparison between numerical results, analytical solutions and experimental results under controlled flow conditions may assist in the accurate selection of flow resistance coefficient. Fourth the simplicity of the equations may allow the extension of the method to non-Newtonian fluids. For example, Chanson et al. (2004) applied successfully the mathematical treatment of Hunt (1982) to dam break wave of non-Newtonian thixotropic fluids. Relevant applications include mud flows, self-flowing concrete and debris flows in civil engineering. Fifth the development may be extended to sloping channels, within some assumptions (Chanson 2005a). Applications include wave runup on upward sloping beach faces and dam break wave on mild slope valleys.

ACKNOWLEDGMENTS

The writer thank all the people who provided him with informations, witness reports, photographs and movies on the 26 December 2004 tsunami, incl. Prof. S. Aoki (TUT) and Dr J. Borrero (SCU).

REFERENCES

Barré de Saint-Venant, A.J.C. (1871). "Théorie et Equations Générales du Mouvement Non Permanent des Eaux Courantes." *Comptes Rendus des séances de l'Académie des Sciences*, Paris, France, Séance 17 July 1871, Vol. 73, pp. 147-154 (in French).

Cavaille, Y. (1965). "Contribution à l'Etude de l'Ecoulement Variable Accompagnant la Vidange Brusque d'une Retenue." *Publ. Scient. et Techn. du Ministère de l'Air*, No. 410, Paris, France, 165 pages (in French).

Chanson, H. (2004). "Environmental Hydraulics of Open Channel Flows." *Elsevier Butterworth-Heinemann*, Oxford, UK, 483 pages (ISBN 0 7506 6165 8).

Chanson, H. (2005a). "Applications of the Saint-Venant Equations and Method of Characteristics to the Dam Break Wave Problem." *Report No. CH55/05*, Dept. of Civil Engineering, The University of Queensland, Brisbane, Australia, May, 135 pages. {http://www.uq.edu.au/~e2hchans/reprints/ch5505.zip}

Chanson, H. (2005b). "Le Tsunami du 26 Décembre 2004: un Phénomène Hydraulique d'Ampleur Internationale. Premier Constats." ('The 26 December 2004 Tsunami: a Hydraulic Engineering Phenomenon of International Significance. First Comments') *Jl La Houille Blanche*, No. 2, pp. 25-32.

Chanson, H., Coussot, P., Jarny, S., and Toquer, L. (2004). "A Study of Dam Break Wave of Thixotropic Fluid: Bentonite Surges down an Inclined Plane." *Report No. CH54/04*, Dept. of Civil Engrg., Univ. of Queensland, Brisbane, Australia, 90 pages.

Chanson, H., Aoki, S., and Maruyama, M. (2000). "Unsteady Two-Dimensional Orifice Flow: an Experimental Study." *Coastal/Ocean Engineering Report*, No. COE00-1, Dept. of Architecture and Civil Eng., Toyohashi University of Technology, Japan, 29 pages.

Debiane, K. (2000). "Hydraulique des Ecoulements Laminaires à Surface Libre dans une Canal pour des Milieux Visqueux ou Viscoplastiques: Régimes Uniformes, Graduellement Varié, et Rupture de Barrage." *Ph.D. thesis*, University of Grenoble I, Rheology Laboratory INPG-UJF-CNRS, France, 273 pages.

Dressler, R.F. (1952). "Hydraulic Resistance Effect upon the Dam-Break Functions." *Jl of Research, Natl. Bureau of Standards*, Vol. 49, No. 3, pp. 217-225.

Dressler, R. (1954). "Comparison of Theories and Experiments for the Hydraulic Dam-Break Wave." *Proc. Intl Assoc. of Scientific Hydrology Assemblée Générale*, Rome, Italy, Vol. 3, No. 38, pp. 319-328.

Estrade, J. (1967). "Contribution à l'Etude de la Suppression d'un Barrage. Phase Initiale de l'Ecoulement." *Bulletin de la Direction des Etudes et Recherches*, Series A, Nucléaire, Hydraulique et Thermique, EDF Chatou, France, No. 1, pp. 3-128 (in French).

Faure, J., and Nahas, N. (1961). "Etude Numérique et Expérimentale d'Intumescences à Forte Courbure du Front." *Jl La Houille Blanche*, No. 5, pp. 576-586. Discussion: No. 5, p. 587 (in French).

Henderson, F.M. (1966). "Open Channel Flow." *MacMillan Company*, New York, USA.

Hunt, B. (1982). "Asymptotic Solution for Dam-Break Problems." *Jl of Hyd. Div.*, Proceedings, ASCE, Vol. 108, No. HY1, pp. 115-126.

Lauber, G. (1997). "Experimente zur Talsperrenbruchwelle im glatten geneigten Rechteckkanal." *Ph.D. thesis*, VAW-ETH, Zürich, Switzerland (in German).

Liggett, J.A. (1994). "Fluid Mechanics." *McGraw-Hill*, New York, USA.

Montes, J.S. (1998). "Hydraulics of Open Channel Flow." *ASCE Press*, New-York, USA, 697 pages.

Ritter, A. (1892). "Die Fortpflanzung der Wasserwellen." *Vereine Deutscher Ingenieure Zeitswchrift*, Vol. 36, No. 2, 33, 13 Aug., pp. 947-954 (in German).

Schoklitsch, A. (1917). Über Dammbruchwellen." *Sitzungberichten der Königliche Akademie der Wissenschaften, Vienna*, Vol. 126, Part IIa, pp. 1489-1514.

Synolakis, C.E. (1987). "The Run-up of Solitary Waves." *Jl of Fluid Mech.*, Vol. 195, pp. 523-545.

Tsuji, Y. (2005). "Distribution of the Tsunami Heights of the 2004 Sumatra Tsunami in Banda Aceh measured by the Tsunami Survey Team." *Internet Resource* {http://www.eri.u-tokyo.ac.jp/namegaya/sumatera/surveylog/eindex.htm}.

Whitham, G.B. (1955). "The Effects of Hydraulic Resistance in the Dam-Break Problem." *Proc. Roy. Soc. of London*, Ser. A, Vol. 227, pp. 399-407.